Direct Insight into Grain Boundary Reconstruction in Polycrystalline Cu(In, Ga)Se_2 with Atomic Resolution

Daniel Abou-Ras,[1,*] Bernhard Schaffer,[2,3] Miroslava Schaffer,[2,4] Sebastian S. Schmidt,[1] Raquel Caballero,[5] and Thomas Unold[1]

[1]*Helmholtz-Zentrum Berlin für Materialien und Energie, Hahn-Meitner-Platz 1, 14109 Berlin, Germany*
[2]*SuperSTEM, STFC Daresbury Laboratories, Keckwick Lane, Warrington, WA4 4AD, United Kingdom*
[3]*SUPA School of Physics and Astronomy, University of Glasgow, Glasgow, G12 8QQ, United Kingdom*
[4]*Department of Engineering, University of Liverpool, George Holt Building, Ashton Street, Liverpool, L69 3BX, United Kingdom*
[5]*Helmholtz-Zentrum Berlin für Materialien und Energie, Hahn-Meitner-Platz 1, 14109 Berlin, Germany; now at: Universidad Autónoma de Madrid, Módulo 12, C/Francisco Tomás y Valiente 7, 28049 Madrid, Spain*

(Received 27 October 2011; published 15 February 2012)

This work presents results from high-resolution scanning transmission electron microscopy and electron energy-loss spectroscopy on twin boundaries (TBs) and nontwin grain boundaries (GBs) in Cu(In, Ga)Se_2 thin films. It is shown that the atomic reconstruction is different for different symmetries of the grain boundaries. We are able to confirm the model proposed by Persson and Zunger [Phys. Rev. Lett. **91**, 266401 (2003)] for Se-Se-terminated $\Sigma 3$ {112} TBs, showing Cu depletion and In enrichment in the two atomic planes closest to the TB. On the contrary, Cu depletion without In enrichment is detected for a cation-Se-terminated TB. At nontwin GBs, always a strong anticorrelation of Cu and In signals is detected suggesting that the formation of In_{Cu} or Cu_{In} antisites within a very confined region of smaller than 1 nm is an essential element in the reconstruction of these GBs.

DOI: 10.1103/PhysRevLett.108.075502 PACS numbers: 61.72.Mm, 68.37.Ma, 79.20.Uv, 88.40.jn

Solar cells based on Cu(In, Ga)Se_2 thin-film absorbers have reached power-conversion efficiencies of more than 20% [1] in spite of their polycrystalline character. It has been a debate for several years now what the properties of the grain boundaries (GBs) in these thin films are. Experimental results obtained by transport measurements [2] and surface-sensitive, scanning probe techniques [3] suggested that GBs in polycrystalline Cu(In, Ga)Se_2 thin films are, as found in microcrystalline, *p*-type Si [4], positively charged, which leads to down-bending of conduction and valence bands at the GBs, acting effectively as hole barriers. In particular, for large band bending such that the GBs become type-inverted, i.e., that the electrons become majority carriers, the recombination at GBs may be significantly reduced. Two-dimensional device modeling [5–7] showed, however, that such a bend bending at the GBs leads to a reduction in the open-circuit voltage and is thus not beneficial to the overall device efficiency.

Persson and Zunger [8,9] proposed a lowering of the valence-band maximum (VBM) at grain boundaries, acting as a barrier for holes in the grain interiors, thus reducing recombination through defects at the GB. In their calculations by first principles density functional theory, these authors modeled GBs in $CuInSe_2$ and $CuGaSe_2$ as being formed by two polar {112} surfaces, which are considered more stable than nonpolar surfaces in $CuInSe_2$ and $CuGaSe_2$ because of the low formation energies for surface reconstruction. This reconstruction involves generation of either Cu vacancies at cation-cation terminated surfaces or In-on-Cu antisites at the subsurfaces of the Se-{112} planes (Se-Se termination). In case of a surface reconstructed by Cu vacancies, a lowering of the VBM is found. The VBM of $CuInSe_2$ consists of antibonding Se-*p* and Cu-*d* hybrid orbitals. The removal of Cu from the surface results in a lowering of the antibonding state and thus in a lowering of the VBM. In contrast, the VBM is not changed substantially at Se-Se-terminated GBs [9].

Surface-sensitive, experimental studies have shown Cu depletion and In enrichment at GBs in polycrystalline Cu(In, Ga)Se_2 thin films [10], whereas bulk-sensitive analyses have so far not reported any changed composition [11,12]. The disagreement of these results may be due to different GB properties on surfaces (Ref. [10]) and in the volumes of Cu(In, Ga)Se_2 thin films (Refs. [11,12]), which is discussed in more detail elsewhere [13].

In the present work, we provide direct evidence for In-on-Cu antisites in the case of Se-Se-terminated twin boundaries (TBs) with {112} GB planes by applying high-resolution scanning transmission electron microscopy (HR-STEM) combined with electron energy-loss spectrometry (EELS) on identical sample positions. Moreover, we report compositional changes at nontwin GBs and discuss the different changes in composition we found at TBs and nontwin GBs by different reconstruction.

The samples studied for the present work comprise Cu(In, Ga)Se_2 thin films, about 1.9 μm thick, which were deposited on Mo-coated soda-lime glass via multistage coevaporation [14]. These Cu(In, Ga)Se_2 thin films exhibited compositional ratios of $[Cu]/([In]+[Ga]) = 0.70 \pm 0.03$ and of $[Ga]/([In]+[Ga]) = 0.31 \pm 0.02$ as

measured by means of x-ray fluorescence analyses. The solar cells were completed by chemical bath deposition of a CdS buffer layer (approximately 50 nm thick) and an rf-sputtered ZnO/ZnO:Al bilayer front contact (80 nm/400 nm).

Specimens for HR-STEM and EELS analyses were prepared from working devices using a FEI Helios NanoLab 600 DualBeam focused-ion beam (FIB) machine. Acceleration voltages of down to only 500 V were applied for the Ga-ion beam of the FIB machine, in order to reduce possible measurement artifacts or compositional changes in the specimen to a minimum [15]. The HR-STEM images and the EELS data were acquired using a NION UltraSTEM 100 microscope at a spot size of 0.08 nm equipped with a Gatan ENFINA spectrometer for EELS measurements. Spectra were acquired at a 1 eV/channel dispersion covering the energy-loss range from 300 to 1640 eV.

Within the $Cu(In, Ga)Se_2$ thin film in the $ZnO/CdS/Cu(In, Ga)Se_2/Mo$ glass stack studied for the present work, $\Sigma 3$ [16] TBs and non-$\Sigma 3$ GBs, which will be termed random in the following, were identified in HR-STEM images. By means of spatially resolved EELS measurements, the elemental occupations of the individual atomic columns were determined. We divided the TBs into three categories: two with Se-Se terminated {112} lattice planes (type I and II), and one with a cation-containing {112} plane facing a Se {112} plane (type III), see Fig. 1 for an overview. Cation-cation terminated TBs were not identified in the sample studied. It is apparent from the HR-STEM images in Fig. 1 that the distances between the atomic planes adjacent to the twin-boundary planes are larger for the type I and II twins (0.28 ± 0.01 and 0.29 ± 0.01 nm, while 0.20 ± 0.01 nm at the type III TB; the errors were estimated as systematic from various measurements). This difference in distance can be attributed to different Se-Se and Se-cation bonding lengths across the type I, II, and III TBs.

Elemental distribution maps composed of Cu, In, and Se signals extracted from individual EEL spectra acquired on an area containing a TB of type I (Fig. 1) are given in Fig. 2. It was not possible to evaluate the Ga-$L_{2,3}$ edge since it was superimposed by the Cu-$L_{2,3}$ edge in the EEL spectrum. Na and oxygen signals do not exhibit intensities above the noise level. While the Se signal distribution [Fig. 2(b)] corresponds well to the atomic lattice image given in Fig. 2(a), the In and Cu distributions appear smeared out, suggesting interdiffusion of these atoms. Nevertheless, substantial Cu depletion and slight In enrichment is found at the position of the TB [Figs. 2(c) and 2(d)], compared with the grain interiors, as illustrated by the line scan given in Fig. 2(e).

Corresponding HR-STEM and EELS measurements at the type II TB (see Supplemental Material [17]) agree well with the results from the type I TB. In contrast, no considerable In enrichment (as compared with the Se signal) but

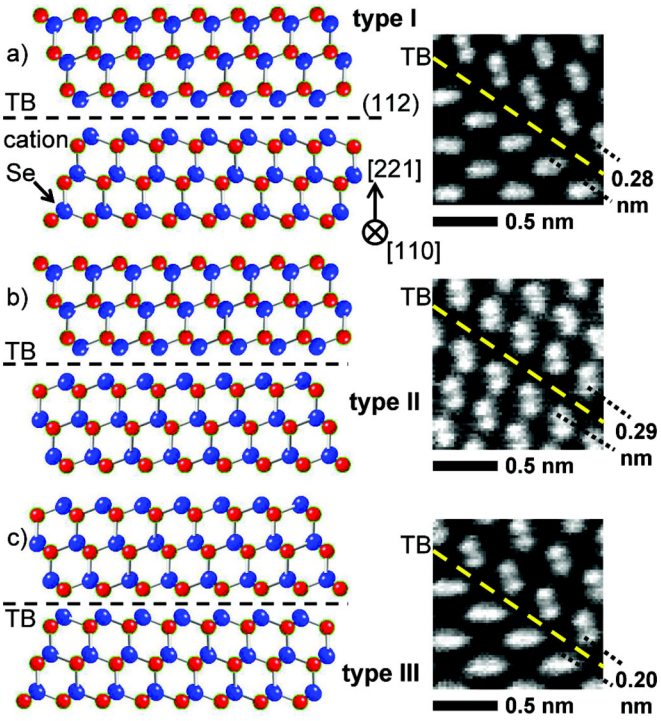

FIG. 1 (color online). Structural representations of the TBs analyzed for the present work and the corresponding high-resolution STEM images (type I, II, and III). The positions of the Se and cation columns were determined from EELS measurements (by Figs. 2 and 3; see also Supplemental Material [17]).

indeed also Cu depletion was detected at the type III TB (Fig. 3). As found for the type I and II TBs, Na and oxygen signals exceeding the noise level were not measured. This result of Cu depletion and In enrichment at type I and II TBs is a direct, experimental evidence for the model given by Persson and Zunger [8,9], which assumes reconstruction of such TBs by the formation of Cu vacancies and In_{Cu} antisite defects. Since {112} planes contain both, Cu and In (and Ga) atoms, the finding of reduced Cu and enhanced In signals cannot be explained by geometrical aspects at the TB but only by atomic reconstruction. As suggested by the reduced Cu signal at the type III TB, reconstruction of internal surfaces via formation of Cu vacancies also takes place in case of oppositely charged polar surfaces (type III TB).

We note that the region of compositional changes at the TBs is very narrow, only of approximately 0.7–0.8 nm in width, corresponding well to about twice the interplanar distances of {112} planes in $Cu(In, Ga)Se_2$ crystals (about 0.33 nm; for type I and II TBs, taking into account also the gap between the Se-containing {112} planes, about 0.08–0.09 nm, see Fig. 1). In a previous work, Hafemeister *et al.* [18] reported about the transport properties across a $\Sigma 3$ TB in $CuGaSe_2$ and were able to simulate conductivity and Hall measurements by taking into account tunneling of holes across a 2 nm wide and 170 meV deep barrier at the TB, formed by a lowered

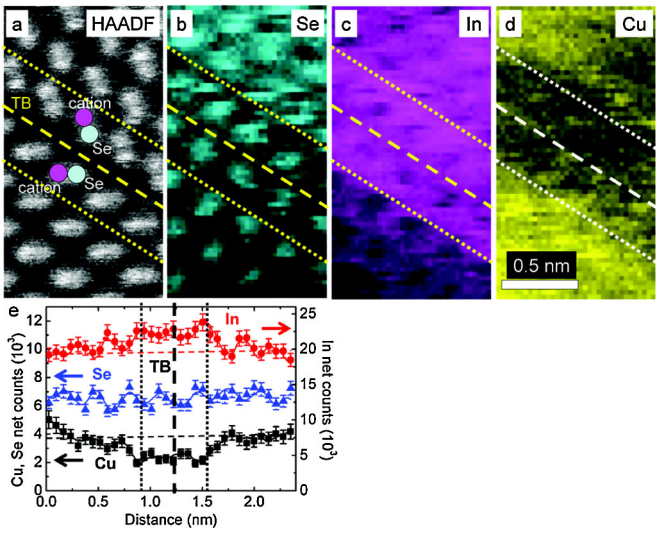

FIG. 2 (color online). High-resolution STEM image (a) of the Se-Se-terminated TB given in Fig. 1(a), as well as Se, In, and Cu distribution maps [(b), (c), and (d)] extracted from EELS spectra acquired on the identical area as the STEM image. An EELS line scan acquired across this TB at yet a different position (e) exhibits substantial Cu depletion and slight In enrichment at the position of the TB. Dotted lines in (a)–(e) indicate the limits of the region around the TB where changes in composition were detected. Dashed horizontal lines in (e) give the level of the Se signal, which was taken as reference. The error bars were estimated from the systematic errors at 10% of the measured values.

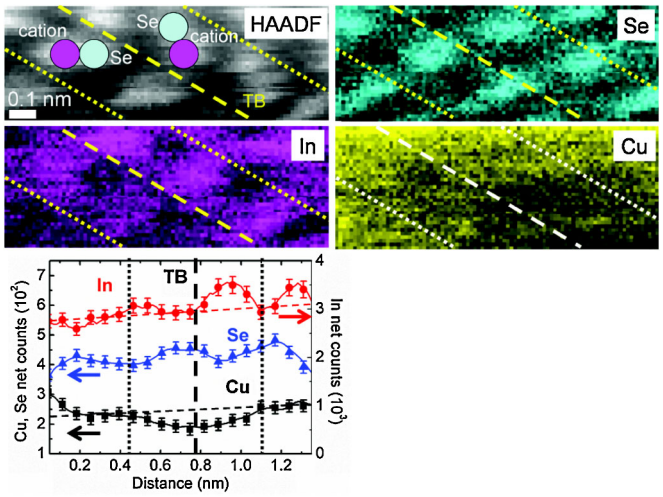

FIG. 3 (color online). High-resolution STEM image of the Se-cation-terminated TB given in Fig. 1(c), as well as In, Se, and Cu distribution maps extracted from EELS spectra acquired on the identical area as the STEM image. The elemental distribution profiles were extracted from across the maps. Dotted lines in the STEM image, the maps, and the profiles indicate the limits of the region around the TB where changes in composition were detected. Dashed horizontal lines give the level of the Se signal, which was taken as reference. The error bars were estimated from the systematic errors at 10% of the measured values.

VBM. The width of this suggested barrier is larger than the extensions of the regions at TBs with compositional changes, as measured in the present work. Nevertheless, tunneling of charge carriers to the TB is very probable for widths below 3 nm, as calculated by Taretto *et al.* [7].

Analyses of $\Sigma 3$ TBs by means of electron-beam-induced current (EBIC) [13,19,20] as well as scanning Kelvin probe force microscopy [21], both combined with electron backscatter diffraction on the identical sample positions, showed no sign of considerably reduced short-circuit currents or charge accumulations. Thus, TBs are considered not to affect substantially the device performance of the Cu(In, Ga)Se_2 thin-film solar cell. This may also be related to the results presented by Yan *et al.* [22], who performed *ab initio* calculations for $\Sigma 3$ TBs with {114} TB planes, comparing density of states before and after lattice relaxation. These authors show that after lattice relaxation, the density of deep defect levels in the band gap at these TBs is very low.

Further combined HR-STEM imaging and EELS analyses were performed at random GBs. In contrast to the $\Sigma 3$ TBs, the EELS result obtained at the random GB [Fig. 4(a)] shows Cu and O enrichments as well as In depletion at the position of the GB [Fig. 4(b)]. The Se signal does not change significantly. The region around the GB where compositional changes are detected (about 0.7 nm full width at half maximum) is very narrow. By comparison with the HR-STEM image in Fig. 4(a), this region corresponds well to the two atomic planes closest to the GB (dashed lines).

At yet another (random) GB in the identical Cu(In, Ga)Se_2 thin film (see Supplemental Material [17]), copious Se depletion was found, while the Cu, In, and oxygen signals behave similarly as in Fig. 4(b). Especially in these elemental distribution profiles, the anticorrelations of Cu and In signals as well as of Se and oxygen signals are apparent.

EELS measurements at random GBs in several further Cu(In, Ga)Se_2 thin films with various [Cu]/([In] + [Ga]) ratios confirmed these results, also showing changed compositions at these GBs, with Cu and In signals always being anticorrelated, while Se depletion and O enrichment have been measured only in some cases. Except for these anticorrelations of Cu/In and of Se/O signals, there is not any general trend in compositional changes found at Cu(In, Ga)Se_2 GBs. We have found them to be in part enriched (depleted), and in part also depleted (enriched) in Cu (In). The anticorrelation of Cu and In signals always present at Cu(In, Ga)Se_2 GBs indicates a preferential site exchange of Cu and In atoms, leading to the formation of In_{Cu}^{2+} and Cu_{In}^{2-} antisites. However, also the formation of V_{Cu}^{-} (Cu vacancies) and neutral defect complexes as $(2V_{Cu}^{-} + In_{Cu}^{2+})$ and $(Cu_{In}^{2-} + In_{Cu}^{2+})$ have to be considered [23].

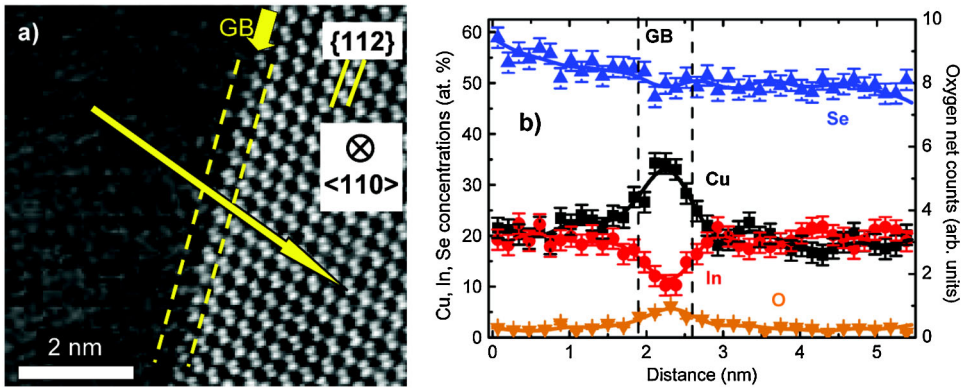

FIG. 4 (color online). High-resolution STEM image (a) of a random (nontwin) GB (indicated by small arrow). EEL spectra were acquired along the large arrow given in (a), and elemental distribution profiles (b) were extracted from these spectra . The region where compositional changes were detected are highlighted by dashed lines. Cu and O enrichments as well as In depletion are found at the position of the GB, while the Se signal does not change significantly. The, Cu, In, and Se signals were quantified by relating the average net counts in the grain interiors to the integral concentrations determined by x-ray fluorescence technique (XRF). The error bars were estimated from the systematic errors at 10% of the measured values.

From the EELS data acquired, we did not detect enhanced Na and O signals at TBs down to the detection limit of about 1 at. %. Enhanced O signals were, in contrast, detected at random GBs by means of EELS. In view of O and further impurities such as Na and K which have been reported to segregate at Cu(In, Ga)Se_2 GBs [24–27], we need to take into account that these impurities may influence the atomic reconstruction at GBs.

Reduced densities of deep defects in the band gap at (probably) random GBs were reported by Mönig *et al.* by surface-sensitive, scanning tunneling spectroscopy [28]. This result suggests that the model by Yan *et al.* [22], which predicts reduced densities of subgap defects at TBs is also valid for random GBs. Reduced densities of subgap states even at random GBs in Cu(In, Ga)Se_2 thin films is a good explanation for the rather small reduction of the short-circuit current of only about 5% (measured by EBIC [13,19,29]), compared with values of about 50% known from multicrystalline Si [30,31] or CdTe thin films [32], and also for the measured low recombination velocities of about 10^4 cm/s [19,33].

In conclusion, atomic reconstructions or redistributions were detected with subnanometer resolution at TBs as well as at random GBs in Cu(In, Ga)Se_2 thin films. We are able to confirm the model proposed by Persson and Zunger [8,9] for Se-Se-terminated $\Sigma 3$ {112} TBs, showing Cu depletion and In enrichment in the two atomic planes closest to the TB. Cu depletion without In enrichment was detected at a Se-cation-terminated $\Sigma 3$ {112} TB. At random grain boundaries, different changes of composition were found at different GBs, while the reconstruction is apparently dominated by a preferential site exchange of Cu and In as well as (in part also) of Se and O atoms.

The authors would like to thank B. Bunn, C. Kelch, M. Kirsch, T. Münchenberg, and H. Kropf for help in solar-cell production and sample preparation, as well as H. W. Schock for fruitful discussions and continuous support. Funding from the German ministry for environment (BMU) under Contract No. 0327559H (German-Israeli project ProGraB) as well as by the ESTEEM project is gratefully acknowledged. B. S. and M. S. thank the EPSRC for funding of the SuperSTEM facility and for the operator times. Special thanks are due to Dr. B. Mendis, Durham University, for providing access to a FIB machine.

*daniel.abou-ras@helmholtz-berlin.de

[1] P. Jackson, D. Hariskos, E. Lotter, W. R. S. Paetel, R. Menner, W. Wischmann, and M. Powalla, Prog. Photovoltaics **19**, 894 (2011).
[2] S. Schuler, S. Nishiwaki, J. Beckmann, N. Rega, S. Brehme, S. Siebentritt, and M. C. Lux-Steiner, in *Conference Records of the IEEE Photovoltaic Specialists Conference* (IEEE, Piscataway, 2002) pp. 504–507.
[3] C.-S. Jiang, R. Noufi, J. A. AbuShama, K. Ramanathan, H. R. Moutinho, J. Pankow, and M. M. Al-Jassim, Appl. Phys. Lett. **84**, 3477 (2004).
[4] J. W. Y. Seto, J. Appl. Phys. **46**, 5247 (1975).
[5] M. Gloeckler, J. R. Sites, and W. K. Metzger, J. Appl. Phys. **98**, 113704 (2005).
[6] W. Metzger and M. Gloeckler, J. Appl. Phys. **98**, 063701 (2005).
[7] K. Taretto and U. Rau, J. Appl. Phys. **103**, 094523 (2008).
[8] C. Persson and A. Zunger, Phys. Rev. Lett. **91**, 266401 (2003).
[9] C. Persson and A. Zunger, Appl. Phys. Lett. **87**, 211904 (2005).
[10] M. J. Hetzer, Y. M. Strzhemechny, M. Gao, M. C. Contreras, A. Zunger, and L. J. Brillson, Appl. Phys. Lett. **86**, 162105 (2005).
[11] Y. Yan, R. Noufi, and M. M. Al-Jassim, Phys. Rev. Lett. **96**, 205501 (2006).

[12] C. Lei, C. M. Li, A. Rockett, and I. M. Robertson, J. Appl. Phys. **101**, 024909 (2007).
[13] S. Sadewasser, D. Abou-Ras, D. Azulay, R. Baier, I. Balberg, D. Cahen, S. Cohen, K. Gartsman, G. Karuppiah, J. Kavalakkatt, W. Li, O. Millo, T. Rissom, Y. Rosenwaks, H.-W. Schock, A. Schwarzman, and T. Unold, Thin Solid Films **519**, 7341 (2011).
[14] C. A. Kaufmann, R. Caballero, T. Unold, R. Hesse, R. Klenk, S. Schorr, M. Nichterwitz, and H.-W. Schock, Solar Energy Mater. Sol. Cells **93**, 859 (2009).
[15] J. Mayer, L. A. Giannuzzi, T. Kamino, and J. Michael, MRS Bull. **32**, 400 (2007); M. Schaffer, B. Schaffer, and Q. Ramasse, Ultramicroscopy (in press).
[16] H. Grimmer, W. Bollmann, and D. H. Warrington, Acta Crystallogr. Sect. A **30**, 197 (1974).
[17] See Supplemental Material at http://link.aps.org/supplemental/10.1103/PhysRevLett.108.075502 for further results from a TB (type II) and a random (nontwin) GB.
[18] M. Hafemeister, S. Siebentritt, J. Albert, M. C. Lux-Steiner, and S. Sadewasser, Phys. Rev. Lett. **104**, 196602 (2010).
[19] M. Nichterwitz, D. Abou-Ras, K. Sakurai, J. Bundesmann, T. Unold, R. Scheer, and H. W. Schock, Thin Solid Films **517**, 2554 (2009).
[20] M. Kawamura, T. Yamada, N. Suyama, A. Yamada, and M. Konagai, Jpn. J. Appl. Phys. **49**, 062301 (2010).
[21] R. Baier, D. Abou-Ras, T. Rissom, M. C. Lux-Steiner, and S. Sadewasser, Appl. Phys. Lett. **99**, 172102 (2011).
[22] Y. Yan, C.-S. Jiang, R. Noufi, S.-H. Wei, H. R. Moutinho, and M. M. Al-Jassim, Phys. Rev. Lett. **99**, 235504 (2007).
[23] S. B. Zhang, S.-H. Wei, A. Zunger, and H. Katayama-Yoshida, Phys. Rev. B **57**, 9642 (1998).
[24] E. Cadel, N. Barreau, J. Kessler, and P. Pareige, Acta Mater. **58**, 2634 (2010).
[25] R. Schlesiger, C. Oberdorfer, R. Wuerz, G. Greiwe, P. Stender, M. Artmeier, P. Pelka, F. Spaleck, and G. Schmitz, Rev. Sci. Instrum. **81**, 043703 (2010).
[26] O. Cojocaru-Miredin, P. Choi, R. Wuerz, and D. Raabe, Ultramicroscopy **111**, 552 (2011).
[27] O. Cojocaru-Miredin, P. Choi, D. Abou-Ras, S. S. Schmidt, R. Caballero, and D. Raabe, IEEE J. Photovolt. **1**, 207 (2011).
[28] H. Mönig, Y. Smith, R. Caballero, C. A. Kaufmann, I. Lauermann, M. C. Lux-Steiner, and S. Sadewasser, Phys. Rev. Lett. **105**, 116802 (2010).
[29] D. Abou-Ras, J. Dietrich, J. Kavalakkatt, M. Nichterwitz, S. S. Schmidt, C. T. Koch, R. Caballero, J. Klaer, and T. Rissom, Solar Energy Mater. Sol. Cells **95**, 1452 (2011).
[30] J. Palm, J. Appl. Phys. **74**, 1169 (1993).
[31] C. Donolato, R. Nipoti, D. Govoni, G. P. Egeni, V. Rudello, and P. Rossi, Mater. Sci. Eng. B **42**, 306 (1996).
[32] M. Terheggen, Ph.D. thesis, ETH Zurich, 2003.
[33] W. K. Metzger, I. L. Repins, M. Romero, P. Dippo, M. Contreras, R. Noufi, and D. Levi, Thin Solid Films **517**, 2360 (2009).